Ab initio potential energy surface and spectrum of the $B(^3\Pi)$ state of the HeI_2 complex

Álvaro Valdés, Rita Prosmiti,[a] Pablo Villarreal, and Gerardo Delgado-Barrio
Instituto de Matemáticas y Física Fundamental, CSIC, Serrano 123, 28006 Madrid, Spain

Hans-Joachim Werner
Institut für Theoretische Chemie, Universität Stuttgart, Pfaffenwaldring 55, D-75069 Stuttgart, Germany

(Received 7 March 2007; accepted 16 April 2007; published online 22 May 2007)

The three-dimensional interaction potential for $I_2(B\ ^3\Pi_{0_u^+})+He$ is computed using accurate *ab initio* methods and a large basis set. Scalar relativistic effects are accounted for by large-core relativistic pseudopotentials for the iodine atoms. Using multireference configuration interaction calculations with subsequent treatment of spin-orbit coupling, it is shown for linear and perpendicular structures of the complex that the interaction potential for $I_2(B\ ^3\Pi_{0_u^+})+He$ is very well approximated by the average of the $^3A'$ and $^3A''$ interaction potentials obtained without spin-orbit coupling. The three-dimensional $^3A'$ and $^3A''$ interaction potentials are computed at the unrestricted open-shell coupled-cluster level of theory using large basis sets. Bound state calculations based on the averaged surface are carried out and binding energies, vibrationally averaged structures, and frequencies are determined. These results are found to be in excellent accord with recent experimental measurements from laser-induced fluorescence and action spectra of HeI_2. Furthermore, in combination with a recent *X*-state potential, the spectral blueshift is obtained and compared with available experimental values. © *2007 American Institute of Physics*. [DOI: 10.1063/1.2737782]

I. INTRODUCTION

In recent years *ab initio* electronic structure calculations have advanced to a point that they are useful for determining accurate potential energy surfaces (PESs) for rare gas-dihalogen van der Waals (vdW) species.[1–6] So far, the majority of the *ab initio* studies of such complexes was focused on the topology of the ground PESs, which was found to be more anisotropic than expected. There are only few *ab initio* results for the excited electronic states. Recently, *ab initio* calculations have been reported for the *B* states of the $He-Cl_2$ (Ref. 2) and $He-Br_2$ (Ref. 7) systems. For $He-Cl_2$ these potentials have been used in $B\leftarrow X$ dynamics simulations, while only semiempirical potentials were used in theoretical studies of the *B*-state dynamics of other similar systems.[8,9] The experimental data available on the structure and dynamics of these systems originate mainly from $B\leftarrow X$ excitation spectroscopy.[10–12]

To accurately model the dynamics of an open-shell system, one has to account for spin-orbit effects, which leads to an interaction of different adiabatic states. *Ab initio* electronic structure calculations that incorporate the spin-orbit interaction have been presented recently for the $NeCl_2$ *B*-state complex.[13] The electronic mixing has been considered at three selected angular configurations, and a new mechanism has been proposed for electronic energy transfer from highly vibrationally excited *B*-state levels. For an accurate dynamics treatment, several global potential energy and spin-orbit coupling surfaces would be required in this case. Such calculations as well as first principles dynamics simulations that incorporate all coupling effects still remain a challenge for open-shell systems, particularly for the ones containing heavy halogen atoms.

The HeI_2 vdW cluster has been extensively studied by Levy and co-workers.[14,15] By resolving the rotational structure of the fluorescence excitation spectrum of the $B\leftarrow X$ transition, the structure of the complex has been determined for both electronic states. Spectral blueshifts and predissociation linewidths for low and high v levels[15,16] have also been measured for the *B* state by frequency-resolved experiments. Time-resolved experiments carried out by Gutmann *et al.*[17] yielded vibrational predissociation lifetimes for a range of low v levels. Other data available are the *X* and *B* binding energies,[15,18] which were inferred from the product distributions of vibrational predissociation in the *B* excited state. In addition, recent experimental studies by Loomis and coworkers of the $B\leftarrow X$ spectrum have shown that the spectral features are associated with transitions of multiple conformers of several $He-XY$ complexes,[11,12] and binding energies and structures of the ground and *B* excited state isomers have been reported for $He-I_2$.[19]

A direct comparison with experiment requires theoretical PESs of the same quality for both electronic states involved. To our knowledge, there is so far no *ab initio* calculation of PES of the $HeI_2(B)$ complex. Only recently, a three-dimensional *ab initio* CCSD(T) PES has been reported for the ground $HeI_2(X)$ complex.[20] In this work we present calculations of the $HeI_2(B)$ interaction potential. We use the supermolecular approach and the spin unrestricted open-shell coupled-cluster [ROHF-UCCSD(T)] method. Scalar relativ-

[a]Electronic mail: rita@imaff.cfmac.csic.es

istic effects are included by using large-core pseudopotentials for the I atoms, and large augmented correlation consistent polarized basis sets are employed to ensure convergence of the interaction energies. As will be discussed in the next section, spin-orbit coupling effects can be accurately accounted for by averaging the $^3A'$ and $^3A''$ interaction potentials. The new *ab initio B*-state PES, in combination with the CCSD(T) *X*-state PES, will allow us to make a first comparison with data obtained by experimental measurements.

II. COMPUTATIONAL METHODS AND RESULTS

A. *Ab initio* electronic structure calculations

All *ab initio* calculations have been performed with the MOLPRO program.[21] We use Jacobi coordinates (r,R,θ) to describe the PES for the HeI_2 complex, where R is the distance of the He atom from the center of mass of I_2, r is the bond length of I_2, and θ is the angle between the **R** and **r** vectors.

Scalar relativistic effects were accounted for by using relativistic effective core potentials (ECPs) for the I atoms. Two different ECPs, developed by the groups of Stoll and Dolg in Stuttgart have been compared: a large-core potential denoted ECP46MDF,[22] and a small-core potential denoted ECP28MDF.[23] The basis set used in the large-core calculations was optimized for the ECP46MDF potential by Dolg.[22] This basis is of quadruple zeta quality $(7s7p4d3f2g[6s6p4d3f2g])$ and includes diffuse *s*, *p*, and *d* functions. The parameters for the ECP46MDF potential and the associated basis set can be found in the supplementary material.[24] For the small-core calculations, we used the augmented correlation consistent basis sets aug-cc-pVQZ-PP and aug-cc-pV5Z-PP optimized by Peterson. For He, the corresponding aug-cc-pVnZ basis sets[25] were used.

In order to account for core-valence correlation effects, a core polarization potential[26] (CPP) was used in the large-core calculations. The parameters of this potential were[22] (all values in a.u.) $\alpha=1.028$ (core polarizability), $r_c=1.23$ (cut-off radius), and $q=2$ (exponent in cut-off function). For the small-core calculations one would either have to reoptimize these parameters, or to explicitly correlate the 18 additional electrons, using a larger basis set with tight polarization functions. Neither of these possibilities have been attempted in the current work, i.e., core-core and core-valence correlation effects were entirely neglected in the small-core calculations.

The accuracy of the ECPs and associated basis sets and the importance of spin-orbit effects on the interaction potentials was tested using internally contracted multireference configuration interaction (MRCI) calculations.[27–29] The orbitals were optimized in state-averaged complete active space self-consisted-field (CASSCF) calculations,[30,31] and the CASSCF wave functions were used as reference functions in the MRCI. In all cases, a full valence active space (14 electrons in 8 orbitals for I_2 and 16 electrons in 9 orbitals for HeI_2) was used, and all 18 states (9 singlets and 9 triplets) that correlate asymptotically with the $I(^2P)+I(^2P)$ asymptote were included in the state-averaging procedure. Using the resulting orbitals, MRCI calculations were performed for the 18 states. The Davidson correction $(+Q)$ was applied to all energies in order to account approximately for higher excitations and to reduce the size consistency error. For simplicity, we will omit the specification $+Q$ in the following. Only the valence electrons were correlated, as already mentioned above. The spin-orbit matrix elements were computed as described in Ref. 32. The spin-orbit operator was approximated by one-electron ECPs. Finally, the matrix $\mathbf{H}_{el}+\mathbf{H}_{SO}$ was set up in the basis of the 36 spin states and diagonalized in order to obtain the adiabatic spin-orbit eigenstates. Here $\mathbf{H}_{el}$ is a diagonal matrix containing the MRCI energies. Most of the resulting spin-orbit (SO) states are repulsive. In the following, we will only consider the bound $X\ ^1\Sigma_g^+$ and $B\ ^3\Pi_{0_u^+}$ states. For comparison, we also performed ROHF-UCCSD(T) calculations.[33] In these calculations spin-orbit effects were entirely neglected. Since the $^1\Sigma_g^+$ and $^3\Pi_u$ states are the lowest in their symmetries, there is no problem to use single reference coupled-cluster methods around the equilibrium distance. However, at extended bond distances a second configuration becomes increasingly important, and the ROHF-UCCSD(T) energies for the *B* state become unreasonable for bond distances longer than about 3.5 Å.

We first consider the isolated I_2 molecule and demonstrate the effect of the various approximations (ECP, spin orbit, MRCI, and UCCSD(T)) on the spectroscopic constants of the $X\ ^1\Sigma_g^+$ and $B\ ^3\Pi_{0_u^+}$ states. The harmonic and anharmonic vibrational constants ω_e and $\omega_e x_e$, respectively, were computed from the energy derivatives at r_e, obtained from polynomial fits of ninth degree to 12 points. The asymptotic MRCI energies used to evaluate the dissociation energies were computed at a large distance, while the asymptotic UCCSD(T) energies were taken to be twice the energy of an isolated iodine atom. In Table I the results obtained with small- and large-core ECPs are compared with the experimental values.[34] The UCCSD(T) and MRCI values are computed from the energies without spin-orbit coupling; the MRCI+SO ones include spin-orbit coupling. The asymptotic energy of I_2 is split into three equally spaced levels, corresponding to the $I(^2P_{3/2})\times I(^2P_{3/2})$ (16-fold degenerate), $I(^2P_{3/2})\times I(^2P_{1/2})$ (16-fold degenerate), and $I(^2P_{1/2})\times I(^2P_{1/2})$ (4-fold degenerate) asymptotes. The spacing between these levels corresponds to the splitting of the $I(^2P_{3/2})$ and $I(^2P_{1/2})$ states, and using the large-core potential this splitting is computed to be 0.936 eV (exp. 0.942 eV). Thus, the SO coupling lowers the $I(^2P_{3/2})\times I(^2P_{3/2})$ asymptote by 0.624 eV and raises the $I(^2P_{3/2})\times I(^2P_{1/2})$ asymptote by 0.312 eV relative to the energy obtained without SO coupling.

The $X\ ^1\Sigma_g^+$ state correlates with the lowest asymptote, and since the SO coupling has only a rather small effect (−0.08 eV) on the energy at the equilibrium distance, the SO coupling lowers the dissociation energy by 0.54 eV. Correspondingly, the SO effect slightly increases the equilibrium distance and lowers the harmonic vibrational frequency of the *X* state. The *B* state correlates with the $I(^2P_{3/2})\times I(^2P_{1/2})$ asymptote, and in the basis of the 36 valence states it is a pure mixture of the unperturbed degenerate $^3\Pi_x$ and $^3\Pi_y$ states. Thus, a change of the *B*-state potential can

TABLE I. Calculated and experimental spectroscopic constants (Dissociation energies D_e and excitation energy T_e in eV, equilibrium distances r_e in Å, and frequencies in cm^{-1}. The Davidson correction was applied to the MRCI energies.) for the $X\ ^1\Sigma_g^+$ and $B\ ^3\Pi_{0+}$ states of the I_2 molecule.

	ECP46MDF[a] Dolg[a]			ECP28MDF[b] AV5Z-PP[b]			
ECP basis	CCSD(T)	MRCI	MRCI+SO	CCSD(T)	MRCI	MRCI+SO	Expt.[c]
$D_e(X)$	2.103	2.079	1.548	2.006	1.960	1.467	1.556
$D_e(B)$	0.500	0.479	0.459	0.444	0.410	0.392	0.543
T_e	1.603	1.614	2.035	1.562	1.569	1.958	1.955
$r_e(X)$	2.630	2.634	2.648	2.676	2.679	2.693	2.666
$r_e(B)$	2.983	3.024	3.032	3.028	3.077	3.084	3.025
$w_e(X)$	225.5	223.5	214.8	221.2	219.1	211.2	214.50
$w_e(B)$	136.2	119.2	116.9	133.8	114.7	112.5	125.69
$w_e x_e(X)$	0.51	0.53	0.60	0.51	0.53	0.59	0.614
$w_e x_e(B)$	0.58	0.84	0.86	0.59	0.89	0.90	0.764

[a]Reference 22.
[b]Reference 23.
[c]Reference 34.

only arise from the distance dependence of the spin-orbit coupling. Therefore, the SO effect on the equilibrium distance and harmonic vibrational frequency is quite small. The adiabatic excitation energy T_e is raised by 0.38 eV, which is mainly due to the raise of the B-state potential by the SO coupling, as discussed above for the asymptotic energy.

The spectroscopic constants obtained with the large-core potentials and MRCI+SO are in good agreement with the experimental data and previous calculations.[35] For the B state, the equilibrium distance is predicted slightly too long and the harmonic frequency is somewhat too small. In contrary, the UCCSD(T) calculations underestimate r_e and overestimate ω_e by about the same amount. The errors are somewhat larger for the small-core calculations, despite the fact that a very large basis set (aug-cc-pV5Z-PP) has been used. This is almost certainly due to the neglect of core-core and core-valence correlation effects in these calculations (see above). In fact, if the effect of the CPP on the results of the large-core calculations is added to the small-core ones, the agreement with the experimental results improves and becomes comparable to the large-core calculations.

We now turn to the $He-I_2$ interaction energies. The supermolecular method is used for the calculation of the interaction energies $\Delta E(r,R,\theta)=E_{HeI_2}(r,R,\theta)-E_{He}-E_{I_2}(r)$, and the counterpoise (CP) method[36] is used to correct for basis set superposition errors. Since the MRCI method is not size consistent, the interaction energy does not become zero at large distances. Assuming that the size consistency error is independent of R, $\Delta E(r,\infty,\theta)$ is subtracted from all values $\Delta E(r,R,\theta)$ in order to correct for this error. Since the UCCSD(T) method is size consistent, this correction is not necessary for the coupled-cluster calculations.

We will first consider the case without SO coupling. The presence of the He atom lowers the symmetry, and for nonlinear geometries of the complex the two degenerate $^3\Pi_u$ states of I_2 split into two states of $^3A'$ and $^3A''$ symmetries. In the former case, the singly occupied π_g orbital lies in the molecular plane and faces He, while in the latter case it is perpendicular to the plane. In C_{2v} symmetry (T-shaped configurations), the symmetry of the two states becomes $^3A_1$ and $^3B_1$, respectively. The $^3A''$ ($^3B_1$) state can be expected to be more attractive than the $^3A'$ ($^3A_1$) state, since the polarizability of I_2 in the direction of the more diffuse doubly occupied orbital is larger. At linear geometries the two states are degenerate.

In the presence of SO coupling, the two states mix. In the isolated I_2 molecule, the $^3\Pi_{0_u^+}$ wave function can be described as $1/2[(\Pi_x^{(1,1)}-i\Pi_y^{(1,1)})+(\Pi_x^{(1,-1)}+i\Pi_y^{(1,-1)})]$, where the superscripts correspond to the spin eigenvalues (S,M_S). At nonlinear geometries, small contributions of further states arise, but it is still a very good approximation to assume that the wave function can be described as $1/2[(A'^{(1,1)}-iA''^{(1,1)})+(A'^{(1,-1)}+iA''^{(1,-1)})]$. The interaction potential then becomes the average of the spin-orbit free $^3A'$ ($^3A_1$) and $^3A''$ ($^3B_1$) potentials. Figure 1 compares the MRCI potentials for linear and T-shaped geometries (C_{2v}), computed with and without

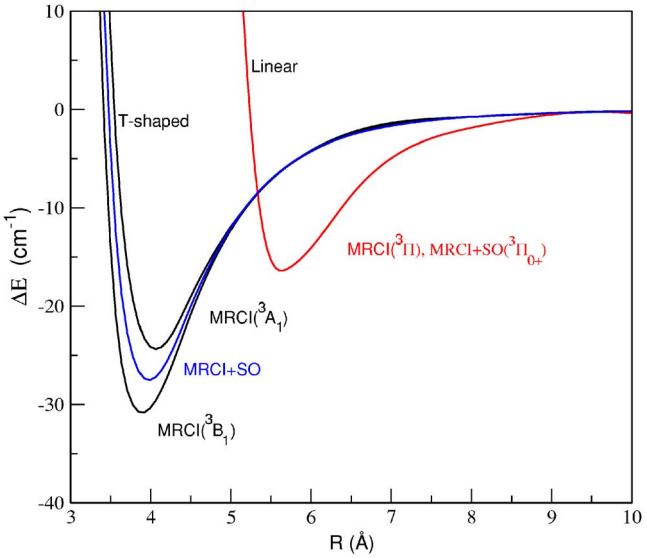

FIG. 1. MRCI potentials with and without spin-orbit coupling for linear and T-shaped configurations of HeI_2 for r=3.024 Å.

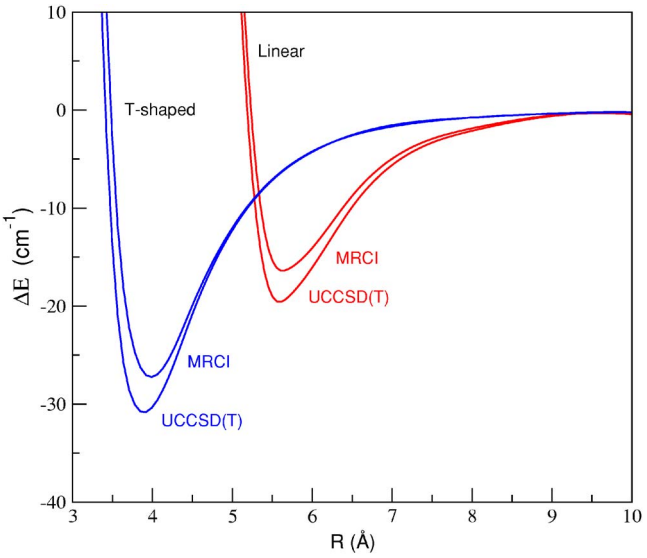

FIG. 2. Comparison of the averaged $^3A'$ and $^3A''$ MRCI and UCCSD(T) interaction potentials for linear and T-shaped configurations of HeI_2 for $r=3.024$ Å.

spin-orbit coupling. At linear geometries, the MRCI+SO $^3\Pi_{0^+}$ interaction potential is virtually identical to the two degenerate MRCI $^3\Pi_x$ and $^3\Pi_y$ potentials. For T-shaped geometries (C_{2v}) the MRCI+SO potential is very close to the average of the MRCI $^3A_1$ and $^3B_1$ potentials. It is therefore an excellent approximation to neglect the spin-orbit coupling entirely and to approximate the interaction potential for the $B\ ^3\Pi_{0_u^+}$ state by the average of the $^3A'$ and $^3A''$ potentials. This approach will be used in the remainder of this paper.

In Fig. 2 the averaged MRCI and UCCSD(T) interaction potentials are compared, again for linear and T-shaped geometries. It is found that the UCCSD(T) well depths are significantly lower than the MRCI ones. This is mainly attributed to the effect of the triple excitations. We therefore decided to use the UCCSD(T) method for all further calculations.

Table II shows a comparison of UCCSD(T) interaction energies for small- and large-core effective core potentials and different basis sets. For the small-core ECPs a series of correlation consistent basis sets are available, and this allows us to extrapolate the energies to the (approximate) complete basis set (CBS) limit. We have performed an extrapolation of the correlation energies using the aug-cc-pVQZ and aug-cc-pV5Z basis sets, assuming $E_n=E_{\mathrm{CBS}}+A/n^3$, where n is the cardinal number. The extrapolated correlation energies were added to the aug-cc-pV5Z Hartree-Fock energies. The extrapolation was performed for all individual energies, and the CP corrected interaction energies were computed thereafter. It is found that the extrapolated interaction energies of the small-core calculations are in very good agreement with the large-core calculation, using aug-cc-pV5Z for He. Due to the different ECPs and basis sets, and the neglect of core-valence correlation in the small-core calculations, this may be somewhat fortuitous. Nevertheless, we decided to perform the final calculations using the large-core ECP, since this is not only computationally more efficient, but also yielded more accurate results for the I_2 spectroscopic constants. Test calculations showed that the g functions of the aug-cc-pV5Z basis for He have only a very small effect (<1 cm^{-1} for the binding energies). Therefore, the final calculations of the potential were performed with the aug-cc-pV5Z(*spdf*) basis for He.

Table II also shows a calculation with the $(3s3p2d2f1g)$ set of bond functions,[37] placed in the middle between He and the center of mass of I_2. Since these functions have no effect on the asymptotic energy, they necessarily lead to a stabilization of the complex. In the current case it appears that the bond functions lead to an overestimation of the binding energy, and therefore they were not considered any further.

Intermolecular energies were calculated for 10–15 R distances ranging from $R=3.35$ to 30 Å. The angle θ was varied between 0° and 90° in steps of 15°, and the I_2 bond lengths were taken to be $r=2.65$, 2.85, 3.024, 3.20, and 3.45 Å. These r values are chosen around the equilibrium distance of $r_e=3.024$ Å and span a range that is large enough to describe the first few excited vibrational levels of $I_2(B)$. The computed UCCSD(T) interaction energies for the A'/A'' states of HeI_2 are listed in the supplementary material.[24] It should be noted that for $r=3.45$ Å and for angular configurations different than the linear and T-shaped ones, we could not achieve convergence in the UCCSD(T) procedure. This

TABLE II. UCCSD(T) interaction energies (in cm^{-1}) for the lowest $^3A_1$ and $^3B_1$ states of He–I_2 obtained with different basis set AVnZ stands for aug-cc-pVnZ, PP for pseudopotential for $r=3.024$ Å and $\theta=90°$ at two distances R.

ECP	Basis		$R=3.75$ Å		$R=4.00$ Å	
I	I	He	$^3A_1$	$^3B_1$	$^3A_1$	$^3B_1$
ECP28MDF	AVQZ-PP	AVQZ	−15.06	−27.50	−23.13	−29.66
ECP28MDF	AV5Z-PP	AV5Z	−17.83	−30.30	−24.86	−31.40
ECP28MDF	CBS[a,b]	CBS[a]	−20.82	−33.23	−26.72	−33.22
ECP46MDF	Dolg[c]	AVQZ	−19.41	−31.30	−25.73	−32.00
ECP46MDF	Dolg	AV5Z	−20.41	−32.34	−26.33	−32.63
ECP46MDF	Dolg	AVQZ+bf[d]	−23.86	−36.00	−28.74	−35.17

[a]Reference 45.
[b]Extrapolated from AVQZ and AV5Z values, see text.
[c]Reference 22.
[d]bf stands for a $(3s3p2d2f1g)$ set of bond functions.

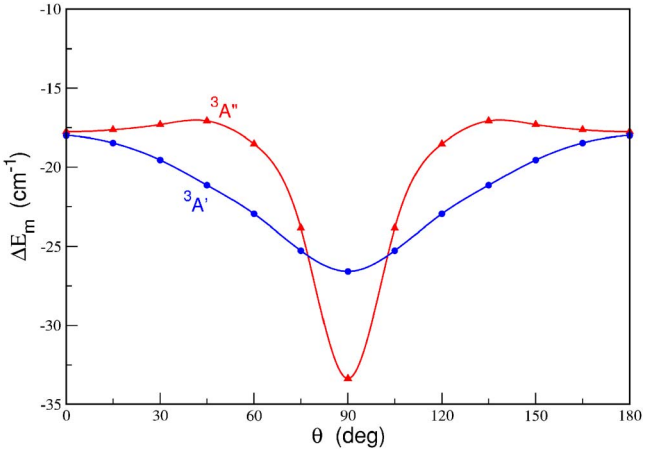

FIG. 3. UCCSD(T) minimum energy paths as a function of θ for the $^3A'$ (circles) and $^3A''$ (triangles) states. r is fixed at r_e=3.024 Å, and R is optimized.

may be related to the strong multireference character of the electronic wave functions at extended I_2 distances.

It is useful to examine the $^3A'/^3A''$ interaction energies for the different I–I bond lengths. For small values of r (2.65 and 2.85 Å) there is only one minimum for the T-shaped structure on both surfaces. For elongated r values (r=3.024, 3.20, and 3.45 Å) the $^3A'$ surface still has only a T-shaped minimum, but the $^3A''$ one has two minima at T-shaped and linear structures. This is similar as for the interaction potential of the $X\,^1\Sigma_g^+$ state.[20] The small barrier between the minima at linear and T-shaped geometries can be attributed to the fact that in the $^3A''$ state the helium atom lies in plane of the doubly occupied π_g orbital. Due to the nodes of this orbital the repulsion should be maximum at intermediate angles, and this seems to overcompensate the attractive dispersion interaction.

Figure 3 shows a comparison of the minimum energy paths as a function of θ for the $^3A'$ and $^3A''$ states for r_e =3.024 Å. The T-shaped configuration is the global minimum of both potentials. The well depths of the fitted $^3A'/^3A''$ surfaces are computed to be 29.64/37.97 for r=2.65 Å, 26.25/33.37 cm^{-1} for r_e=3.024 Å, and 25.52/31.01 for r =3.45 Å. At r=3.024 Å the A'' PES has a shallow well for linear configurations with a dissociation energy of D_e =17.76 cm^{-1} at R=5.7 Å. For an extended I_2 distance of r =3.45 Å the well depth increases to 19.36 cm^{-1} at R =5.8 Å. One should note that as the I–I bond is lengthened the energy difference between the linear and T-shaped wells is decreasing for both states.

B. Representation of potential energy surface and bound state calculations

As noted previously, the $^3A'$ and $^3A''$ states are coupled by spin-orbit interaction. A proper formalism for dynamics calculations is given in Refs. 38 and 39 for scattering and bound states, respectively. In particular, for bound state calculation an effective Hamiltonian, which includes the spin-orbit coupling term, should be employed following the formalism given in Ref. 39. Following Refs. 38–40, the matrix elements of the interaction potential in the atom-diatom case can be represented as the sum or difference of the A' and A'' potentials. In the present case the spin-orbit splitting of the three $I_2(B\,^3\Pi_u)$ states is three to four orders of magnitude larger that the minute difference of the $^3A'$ and $^3A''$ states. Consequently, these states interacting with He atom can be approximated by the sum of the adiabatic states (appropriately modified by spin-orbit coupling) with the difference of the A' and A'' potentials being negligible.

As shown in the previous section, the interaction potential of the B state is very well approximated by the average of the A' and A'' potentials $V_B=(V_{^3A'}+V_{^3A''})/2$, and as in previous studies of similar complexes,[2,7,41] a spin-free closed-shell-type Hamiltonian is employed here to study the nuclear dynamics in the B state.

An analytical functional form based on a Legendre polynomial expansion is chosen to describe the two-dimensional averaged $He-I_2$ interaction potential

$$V_B(R,\theta;r_k)=\sum_{\lambda=0}^{12} V_{k\lambda}(R)P_\lambda(\cos\theta), \quad k=1-4. \tag{1}$$

Due to the symmetry of the system with respect to θ=90° only even terms of λ contribute in the expansion. The $V_{k\lambda}(R)$ coefficients are obtained by a collocation method applying the following procedure. First, for each bond distance r_k (k =1–4) and each angle θ_i (i=1–7), a Morse-vdW function

$$V_B(R;\theta_i;r_k)=\alpha_0^{ik}(\exp(-2\alpha_1^{ik}(R-\alpha_2^{ik}))-2 \times\exp(-\alpha_1^{ik}(R-\alpha_2^{ik})))-\frac{\alpha_3^{ik}}{R^6}-\frac{\alpha_4^{ik}}{R^8} \tag{2}$$

is fitted to the corresponding UCCSD(T) *ab initio* data. The parameters α_0^{ik} α_1^{ik}, α_2^{ik}, α_3^{ik}, and α_4^{ik} are obtained using a nonlinear least square fitting procedure. The resulting values are given in the supplementary material.[24] The coefficients $V_{k\lambda}(R)$ are then obtained by solving the set of Eqs. (1), using the expression of Eq. (2) for each value of θ. This model potential very well reproduces the *ab initio* values, with a maximum standard deviation of 0.026 cm^{-1} and an average standard deviation of 0.015 cm^{-1} for all (r,R,θ) calculated values. Finally, for a three-dimensional (3D) representation of the potential a one-dimensional cubic spline interpolation is employed for the r coordinate.

Figure 4 shows the minimum energy path, V_B^m, as a function of the angle θ for the four r values studied. The interaction energy as well as the anisotropy decrease with increasing bond distance. The global minimum occurs at T-shaped geometries. At the longest bond distance (r =3.2 Å), there is a second local minimum at linear geometries, which is separated from the global minimum by a low barrier.

For the nuclear bound state calculations, the potential is vibrationally averaged using the $I_2(B,v=0)$ vibrational eigenfunction $\chi_v(r)$ with associated eigenvalues $E_{I_2}(v)$. A cubic spline interpolation of the MRCI+SO *ab initio* data (see Table I) is used to represent the $I_2(B)$ potential as a function of r. In Fig. 5 a two-dimensional contour plot of the $V_{v,v}(R,\theta)=\langle\chi_v|V_B(R,\theta,r)|\chi_v\rangle$ surfaces for v=0 as a function of R and θ is presented. The PES has a minimum at θ=90°

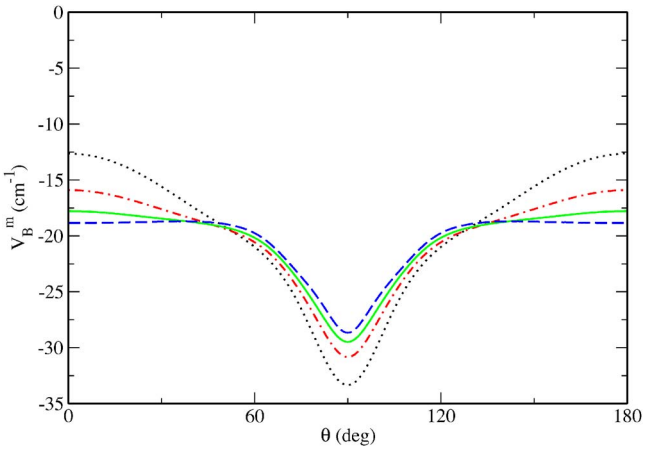

FIG. 4. Minimum energy, V_B^m, in cm^{-1} as a function of θ and r. The dotted, dot-dashed, solid, and long-dashed lines correspond to r=2.65, 2.85, 3.024, and 3.20 Å, respectively.

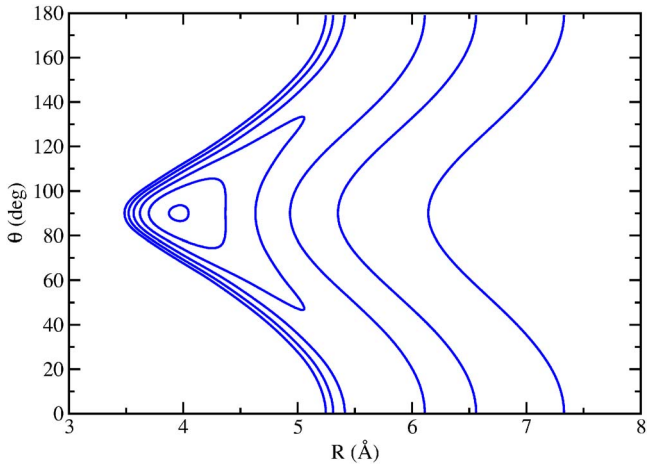

FIG. 5. Contour plots of the vibrationally averaged $V_{v,v}(R,\theta)$ potential for v=0, in the (R,θ) plane. Contour intervals are of 5 cm^{-1} and for energies from −29 to −4 cm^{-1}.

and R=3.96 Å with well depth of 29.41 cm^{-1}.

The rovibrational vdW states are calculated variationally by diagonalizing the vibrationally averaged Hamiltonian $\hat{H}_{v,v}=\langle\chi_{v=0}(r)|\hat{H}|\chi_{v=0}(r)\rangle$

$$\hat{H}_{v,v}=\langle\chi_v|\hat{H}|\chi_v\rangle=-\frac{\hbar^2}{2\mu_1}\frac{\partial^2}{\partial R^2}+\frac{\hat{l}^2}{2\mu_1 R^2}+V_{v,v}(R,\theta)+E_{I_2}(v)+\frac{B_v\hat{j}^2}{\hbar^2}, \quad (3)$$

where $\hat{H}$ is the full spin-free Hamiltonian of HeI_2, B_v is the vibrationally averaged rotational constant of $I_2(B,v)$, $\hat{l}$ is the orbital angular momentum operator of HeI_2, and $\hat{j}$ is the nuclear rotational angular momentum operator of the I_2 diatom, associated with the vectors **R** and **r**, respectively, leading to a total angular momentum $\hat{J}=\hat{l}+\hat{j}$. The reduced masses are calculated using the atomic masses of ^{4}He and ^{127}I isotopes, m_{He}=4.002 60 and m_I=126.904 473 amu, respectively.

The Hamiltonian is represented in a finite three-dimensional basis set. The $V_{v,v}$ potential matrix elements are calculated using a 21-point Gaussian quadrature in the r coordinate, while for the angular coordinate we used a basis of orthonormalized Legendre polynomials $\{P_j(\cos\theta)\}$ with up to 40 values (even and odd) of the diatomic rotation quantum number j. For the radial R coordinate, a basis set of 60 discrete variable representation functions over the range from R=1.75 to 15 Å is used based on the particle in a box eigenfunctions.[42] All calculations are performed for J=0.

In Table III the results of the present calculations are summarized and compared with those of previous theoretical and experimental studies. Direct experimental data are available for the D_0 value of the B state, the energy difference between the first two vibrational levels, E_{01}, as well as for

TABLE III. Experimental and theoretical binding energies D_0 (in cm^{-1}), structures R_0 (in Å), and spectroscopic parameters for the B state of the He–I_2 complex. The structure is T shaped (θ=90°).

	D_0	R_0	E_{01}	D_e	R_e	α	ω_e	$\omega_e x_e$	Blueshift
				UCCSD(T) PES, this work					
2D (v=0)	12.33	4.58	3.97	29.48	3.96	⋯	⋯		2.35
1D	16.26	4.32	14.83	29.72	3.97	1.373	30.96	8.06	⋯
				Semiempirical PES					
1D[a]	14.56	4.38	13.00	26.00	4.0	1.24	26.16	6.58	⋯
1D[b]	23.24	⋯	17.18	36.00	4.0	1.14	28.30	5.56	⋯
2D (v=0)[c]	14.07	⋯	3.85	29.88	3.74	⋯		⋯	3.52
v=20	13.85								
				Expt.					
[d]	13.6–14.8	4.79±0.22	5.66	17.0–18.1	⋯	0.40–0.42	7.02–7.18	0.68–0.76	3.44[e]
[f]	12.8±0.6[g]	⋯	⋯	⋯	⋯	⋯		⋯	3.8[g]

[a]Reference 44.
[b]Reference 45.
[c]Reference 9.
[d]References 14 and 15.
[e]Blueshift value for v=3 (Ref. 14).
[f]Reference 19.
[g]Values for the binding energy of the He–$I_2(B,v=20)$.

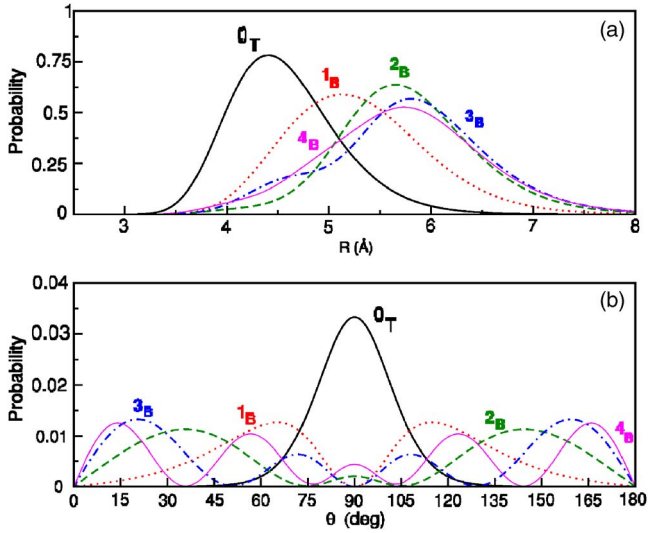

FIG. 6. Radial and angular probability distributions [(a) and (b)] for the indicated n_C vdW levels, calculated using the V_B PES [Eq. (1)]. C is T for T-shaped and B for bending configurations. Angular distributions contain the Jacobian sin θ volume element.

the spectral blueshift with respect to the corresponding band of the uncomplexed iodine molecule,[15,16,43] and for the predissociation linewidths for low and high v levels.[14–17] Based on their experimental data Blazy *et al.* have derived Morse potential parameters for the $He-I_2$ B-state complex,[15] and the intermolecular stretching frequency for the T-shaped well was estimated to be 7.02–7.18 cm^{-1}. Later, Delgado-Barrio and co-workers[44] have suggested, using a sum of Morse pairwise potentials fitted to the experimental vibrational predissociation rates, that the first excited level of the B state and the above frequencies correspond to an excitation of the bending motion. More recently, Gray and Wozny have also presented a semiempirical Morse potential adjusted to reproduce the experimental vibrational predissociation rates of the $HeI_2(B)$ system. In the present work a direct comparison with these semiempirical and experimental data is made by using a one-dimensional Morse potential fitted to the UCCSD(T) data for $\theta=90°$ (see Table III). One can see that the potential parameters and spectroscopic constants obtained from the semiempirical potentials compare very well with the results from the one-dimensional (1D)-UCCSD(T) *ab initio* PES, while the agreement with the experimental parameters is rather poor.

In Table III we also present the results obtained from the two-dimensional bound state calculations using the present vibrationally averaged 3D-UCCSD(T) surface. The results show that the lowest vdW vibrational level ($n=0$) at an energy of −12.33 cm^{-1} corresponds to a T-shaped configuration (see Fig. 6). The next vibrational states are found at energies of −8.36 (odd), −7.58 (even), −6.79 (odd), −5.64 (even), −4.03, (odd) and −2.34(even) cm^{-1}. As can be seen in Fig. 6 the corresponding wave functions are spread over all θ values. In Table IV we compare the above $He+I_2(B,v=0)$ vdW energies with the experimental values reported recently by Ray *et al.*[19] for $He+I_2(B,v=20)$. The agreement is excellent; the computed values are within the experimental uncertainties of ±0.6 cm^{-1} for all energy levels. Furthermore, a vibrationally averaged value $R_0=4.58$ Å is predicted for the T-shaped B-state isomer, which is close to the perpendicular structure with $R_0=4.79\pm0.22$ Å, determined by the analysis of the rotational structure of the $B\leftarrow X$ spectrum.[14]

TABLE IV. Experimental and theoretical energies for the indicated bound vibrational vdW levels of $HeI_2(B,v)$.

n	This work ($v=0$)	Expt. ($v=20$)[a]
0	−12.33	−12.8
1	−8.36	···
2	−7.58	−7.9
3	−6.79	−6.8
4	−5.64	−5.7
5	−4.03	−4.2
6	−2.34	−2.2

[a]Reference 19.

The binding energy value of the B state of HeI_2 has been measured by Blazy *et al.* to be in the range between 13.6 and 14.8 cm^{-1}.[15] Recently, Ray *et al.*[19] determined binding energies of $(12.9-12.7)\pm0.6$ cm^{-1} for the T-shaped $He-I_2(B,v)$, with $v=19-23$. These results are based on their X-state binding energy and the shift of the T-shaped features from the corresponding $I_2(B,v-X,0)$ monomer band origins in the laser-induced fluorescence and action spectra. The values are just outside of the bracketed values reported by Blazy *et al.*[15] and very close (within 0.4 cm^{-1} to the lower bound) to the present estimate of $D_0^B=12.33$ cm^{-1} obtained for the T-shaped $He-I_2(B,v=0)$ complex. It should be noted, however, that the present value is likely to be somewhat too low, since basis set improvements would probably increase the well depth. On the other hand, vibrational excitation of I_2 probably reduces the binding energy, since elongation of the I_2 bond distance reduces the well depth, as seen in Fig. 4.

By analyzing the localization patterns of the corresponding wave functions, one can see in Fig. 6 that the first excited vdW levels correspond mainly to bending excitations. The energy difference E_{01} between the first two vibrational vdW levels is calculated to be $E(n=1)-E(n=0)=3.97$ cm^{-1}, which is smaller than the experimental value of 5.66 cm^{-1} reported by Smalley *et al.*[15,43] We note that the value for the $E(n=1)$ level is not reported by Ray *et al.*,[19] and thus no quantitative comparison with our result is presented here. One can also see in Table III that similar results are obtained for the E_{01} value using a very recent semiempirical two-dimensional (2D) potential.[9] This PES is based on a sum of pairwise He–I Morse functions plus a three body interaction term, adjusted to reproduce successfully both experimental blueshifts and vibrational predissociation lifetimes for $He-I_2(B,v)$ in the range $v=10-67$ of the I_2 vibrational excitations. By comparing now with the results obtained from 1D Morse PES we conclude that, due to the high anharmonicity, a Morse potential is not an appropriate representation of the intermolecular potential of HeI_2 complex.

An estimate of the $B\leftarrow X$ excitation frequency blueshift can be obtained by combining data for the X (Ref. 20) and present B-state potential surfaces. A blueshift value of 3.05 cm^{-1} is calculated as the difference of the $D_0^X-D_0^B$. However, taking into account the Franck-Condon factors,

which strongly favor the transition between the T-shaped $n_X=2$ and $n_B=0$ vdW levels, a value of 2.35 cm^{-1} is predicted for the difference of the $J=0$ energies. This value is somewhat smaller than the experimental value of 3.44 cm^{-1} reported by Blazy *et al.*[15] for $v=3$. Based on the recent experiments by Ray *et al.* we estimate a value of 3.8 cm^{-1} for $v=20$. The experimental D_0^X energies for the T-shaped and linear isomers are very close to each other, 16.6 and 16.3 cm^{-1}, respectively. These values are about 2 and 1 cm^{-1}, respectively, larger than those predicted by the ground state *ab initio* surface[20] employed for the computation of the blueshift. An error of about -1 cm^{-1} in our computed blueshift then means that the binding energy of the B-state potential should be accurate to within about 1 cm^{-1}. This is in line with the direct comparison of the computed and experimental D_0 values of the B state. However, we should note that in order to compare with the experimental values more accurately, one should consider the selection rules for dipole allowed transitions ($\Delta J=0,\pm 1$: $(0\leftrightarrow 0$, $p_X \neq p_B)$, including several total angular momentum J values in the calculations.

III. CONCLUSIONS

We reported *ab initio* calculations on the $I_2(B^3\Pi_{0_u^+})$ +He van der Waals complex. Using MRCI wave functions, it has been shown that the average of the $^3A'$ and $^3A''$ interaction potentials, which correlate with the $^3\Pi_u$ state of I_2, is an excellent approximation for the interaction potential computed with spin-orbit coupling. Therefore, the potential energy surfaces of the $^3A'$ and $^3A''$ state were calculated at the UCCSD(T) level of theory, employing large-core relativistic pseudopotentials for the iodine atoms. The average potential, which has a global minimum at a T-shaped structure, was used in subsequent variational bound state calculations for the complex.

Spin-free bound state calculations for $J=0$ were carried out for the above surface. The binding energy, D_0, is calculated to be 12.33 cm^{-1}. The vibrational ground state wave function is located around the T-shaped structure, and the vibrationally averaged He–I_2 distance is $R_{v=0}=4.58$ Å. These values are in excellent accordance with the recent experiments by Ray *et al.*[19] and earlier experimental measurements by Levy and co-workers.[14,15] The lowest excited bound state levels correspond mainly to the bending motion, and therefore 1D models, which take only into account the stretching coordinate, are unreasonable.

To our knowledge, this is the first *ab initio* study on the B excited state of HeI_2. In combination with a previously computed *ab initio* CCSD(T) potential energy surface for the ground X state the spectral blueshift value for $HeI_2(B,v=0)$ is predicted to be 2.35 cm^{-1}, which compares well with the experimental one of 3.44 cm^{-1}.[15,43] The good agreement means that the X- and B-state binding energies are predicted with comparable accuracy, and *ab initio* calculations for excited states of rare gas-dihalogen vdW molecules can provide data that are useful for the interpretation of experimental data which are related to the location and depth of the potential minima.

For the $HeI_2(B)$ complex more experimental data are available from vibrational predissociation dynamics experiments[15,17] for low and high v excitations. Additionally, experimental studies on the excitation $B\leftarrow X$ spectrum of HeI_2 have been reported recently.[19] In order to simulate these experiments, accurate *ab initio* global potential energy surfaces for a more extended range of bond distances r than reported here are needed. Unfortunately, the single reference UCCSD(T) approximation used in this work breaks down for extended bond distances of I_2. Therefore, more sophisticated multireference methods, such as MRCI, would be needed for such calculations. Furthermore, it is possible that at some geometries the spin-orbit coupling causes strong couplings with other states, as recently found for $NeCl_2$.[13] The theoretical treatment would then require the computation of a large number of states and couplings, and several coupled potentials would have to be included in the dynamics calculations. Such calculations are still beyond the current computational capabilities.

ACKNOWLEDGMENTS

The authors thank Professor M. Dolg for providing the ECPs and basis sets for the large-core calculations. This work has been supported by DGICYT, Spain, Grant No. FIS2004-02461. The authors thank Centro de Calculo (IMAFF), CTI (CSIC), and CESGA for allocation of computer time. One of the authors (A.V.) acknowledges a grant from CICYT, Spain for his stay at Institut für Theoretische Chemie, Universität Stuttgart, Germany. Another author (R.P.) acknowledges support by the Spanish "Ramón y Cajal" Programme, Grant No. PDRyC-2006-001017.

[1] K. Higgins, F.-M. Tao, and W. Klemperer, J. Chem. Phys. **109**, 3048 (1998).
[2] J. Williams, A. Rohrbacher, J. Seong, J. N. Marianayagam, K. C. Janda, R. Burcl, M. M. Szcześniak, G. Chalasiński, S. M. Cybulski, and N. Halberstadt, J. Chem. Phys. **111**, 997 (1999).
[3] F. Y. Naumkin, ChemPhysChem **2**, 121 (2001).
[4] R. Prosmiti, P. Villarreal, and G. Delgado-Barrio, Chem. Phys. Lett. **359**, 473 (2002).
[5] A. Valdés, R. Prosmiti, P. Villarreal, and G. Delgado-Barrio, Chem. Phys. Lett. **357**, 328 (2003).
[6] R. Prosmiti, P. Villarreal, and G. Delgado-Barrio, Isr. J. Chem. **43**, 297 (2003).
[7] M. P. de Lara-Castells, A. A. Buchachenko, G. Delgado-Barrio, and P. Villarreal, J. Chem. Phys. **120**, 2182 (2004).
[8] J. P. Darr, R. A. Loomis, and A. B. McCoy, J. Chem. Phys. **120**, 2677 (2004).
[9] A. Garcia-Vela, J. Chem. Phys. **123**, 124311 (2005).
[10] A. Rohrbacher, J. Williams, and K. C. Janda, Phys. Chem. Chem. Phys. **1**, 5263 (1999).
[11] D. S. Boucher, M. D. Bradke, J. P. Darr, and R. A. Loomis, J. Phys. Chem. A **107**, 6901 (2003).
[12] J. P. Darr, J. J. Clennon, and R. A. Loomis, J. Chem. Phys. **122**, 131101 (2005).
[13] R. Hernández-Lamoneda and K. C. Janda, J. Chem. Phys. **123**, 161102 (2005).
[14] R. E. Smalley, L. Wharton, and D. H. Levy, J. Chem. Phys. **68**, 671 (1978).
[15] J. A. Blazy, B. M. DeKoven, T. D. Russell, and D. H. Levy, J. Chem. Phys. **72**, 2439 (1980).
[16] W. Sharfin, P. Kroger, and S. C. Wallace, Chem. Phys. Lett. **85**, 81 (1982).
[17] M. Gutmann, D. M. Willberg, and A. H. Zewail, J. Chem. Phys. **97**, 8037 (1992).

[18] D. G. Jahn, S. G. Clement, and K. C. Janda, J. Chem. Phys. **101**, 283 (1994).
[19] S. E. Ray, A. B. McCoy, J. J. Glennon, J. P. Darr, E. J. Fesser, J. R. Lancaster, and R. A. Loomis, J. Chem. Phys. **125**, 164314 (2006).
[20] R. Prosmiti, A. Valdés, P. Villarreal, and G. Delgado-Barrio, J. Phys. Chem. A **108**, 6065 (2004).
[21] H.-J. Werner, P. J. Knowles, M. Schtz *et al.*,MOLPRO, version 2002.6, a package of *ab initio* programs, Birmingham, UK, 2003.
[22] M. Dolg, Habilitationsschrift, Universität Stuttgart, 1997.
[23] K. A. Peterson, D. Figgen, E. Goll, H. Stoll, and M. Dolg, J. Chem. Phys. **119**, 11113 (2003).
[24] See EPAPS Document No. E-JCPSA6-126-305721 for the computed interaction energies and fitting coefficients. This document can be reached via a direct link in the online article's HTML reference section or via the EPAPS homepage (http://www.aip.org/pubservs/epaps.html).
[25] R. A. Kendall, T. H. Dunning, Jr., and R. J. Harrison, J. Chem. Phys. **96**, 6796 (1992).
[26] W. Müller, J. Flesch, and W. Meyer, J. Chem. Phys. **80**, 3297 (1984).
[27] H.-J. Werner and P. J. Knowles, J. Chem. Phys. **89**, 5803 (1988).
[28] P. J. Knowles and H.-J. Werner, Chem. Phys. Lett. **145**, 514 (1988).
[29] P. J. Knowles and H.-J. Werner, Theor. Chim. Acta **84**, 95 (1992).
[30] H.-J. Werner and P. J. Knowles, J. Chem. Phys. **82**, 5053 (1985).
[31] P. J. Knowles and H.-J. Werner, Chem. Phys. Lett. **115**, 259 (1985).
[32] A. Berning, M. Schweizer, H.-J. Werner, P. J. Knowles, and P. Palmieri, Mol. Phys. **98**, 1823 (2000).
[33] P. J. Knowles, C. Hampel, and H.-J. Werner, J. Chem. Phys. **99**, 5219 (1993).
[34] K. P. Huber and G. Herzberg, *Constants of Diatomic Molecules*, Molecular Spectra and Molecular Structure Vol. IV (Van Nostrand, Princeton, NJ, 1979).
[35] W. A. de Jong, L. Visscher, and W. C. Nieuwpoort, J. Chem. Phys. **107**, 9046 (1997).
[36] S. F. Boys and F. Bernardi, Mol. Phys. **19**, 553 (1970).
[37] S. M. Cybulski and R. R. Toczylowski, J. Chem. Phys. **111**, 10520 (1999).
[38] M. H. Alexander, Chem. Phys. **92**, 337 (1985).
[39] M.-L. Dubernet, D. Flower, and J. M. Hutson, J. Chem. Phys. **94**, 7602 (1991).
[40] R. J. Doyle, D. M. Hirst, and J. M. Hutson, J. Chem. Phys. **125**, 184312 (2006).
[41] D. S. Boucher, D. B. Strasfeld, R. A. Loomis, J. M. Herbert, S. A. Ray, and A. B. McCoy, J. Chem. Phys. **123**, 104312 (2005).
[42] J. T. Muckerman, Chem. Phys. Lett. **173**, 200 (1990).
[43] R. F. Smalley, L. Wharton, and D. H. Levy, J. Chem. Phys. **64**, 3266 (1976).
[44] J. A. Beswick, G. Delgado-Barrio, and J. Jortner, J. Chem. Phys. **70**, 3895 (1979); J. A. Beswick and G. Delgado-Barrio, *ibid.* **73**, 3653 (1980).
[45] S. K. Gray and C. E. Wozny, J. Chem. Phys. **94**, 2817 (1991).